J. Plasma Physics (2011), *vol.* 77, *part* 4, *pp.* 469–478. © Cambridge University Press 2010 469
doi:10.1017/S0022377810000620

On the inertia term in the momentum equation in the free-fall regime of discharge maintenance

ST. ST. LISHEV[1], A. P. SHIVAROVA[1] and KH. TS. TARNEV[2]

[1]Faculty of Physics, Sofia University, BG-1164 Sofia, Bulgaria (ashiva@phys.uni-sofia.bg)

[2]Department of Applied Physics, Technical University-Sofia, BG-1000 Sofia, Bulgaria

(Received 24 July 2010; accepted 25 September 2010; first published online 27 October 2010)

Abstract. The study, being on two-dimensional modelling of low pressure discharges, suggests an approach to the nonlinear inertia term in the momentum equation of the positive ions needed to be accounted for in the free-fall regime of the discharge maintenance. On the basis of conclusions that the inertia term acts in the wall sheath, where the ions fly perpendicularly to the walls, it is shown that (i) the parallel – to the walls – velocity component can be neglected, and (ii) the rest of the convective derivative can be determined by using the energy conservation law in the collisionless case. In a way, the inertia term acting as a retarding force is joined to the momentum loss term by introducing effective collision frequencies. The validity of the procedure is proved in a model of a low pressure argon discharge by comparison with the exact solutions for the two-dimensional spatial distribution of the discharge characteristics (ion velocity, electron density and temperature and DC electric field and its potential). The conclusion is that (i) ignoring the velocity component that is parallel to the walls does not cause deviation from the exact solution, and (ii) the approximation of using the energy conservation law in the collisionless case is good enough.

1. Introduction

As it is known, the importance of the directed motion due to the formation of well-pronounced wall sheaths in the free-fall regime-sustained discharges requires accounting for the nonlinear inertia term in the momentum equation of the positive ions. This breaks the drift–diffusion approximation used in the description of diffusion-controlled discharges because – with the convective derivative present – the momentum equation of the positive ions appears as a differential equation. Although the arising complications, the one-dimensional (1D) discharge modelling of the free-fall regime-sustained discharges has been successfully developed in the years by presenting different approaches and results for the behaviour of discharges in different gasses, with one or more types of positive ions [1–9].

Introducing an effective electric field is considered as a manner for overcoming the complications due to accounting for the inertia term in the two-dimensional (2D) discharge modelling [10]. The procedure generalizes earlier studies [11, 12] where an effective electric field has been used; however, for accounting for the time derivative in the momentum equation of the positive ions. In a way, the convective derivative in the momentum equation of the positive ions is joined to the drift term (drift in the DC electric field) and the DC electric field is replaced by an effective electric field. This permits formation of an expression for a drift–diffusion flux (needed for the continuity equation) by introducing an equation for the effective electric field in the initial set of equations.

This study suggests another approach to dealing with the nonlinear inertia term in the 2D modelling of low pressure discharges. Results for the plasma parameters obtained with exact account for the nonlinear inertia term in the momentum equation for the positive ions are compared with results obtained in two consecutive approximations. Ignoring the parallel — to the corresponding wall — velocity component in the inertia term is the first approximation shown not to cause deviation from the exact solution. The reason is that the inertia term appears to act in the wall sheath where the ions fly almost perpendicularly to the corresponding wall. For determination of the spatial derivative of the velocity in the rest of the inertia term, the energy conservation law in the collisionless case is used. This is the second approximation, shown to be good enough. It permits to add the inertia term to the momentum loss term and to introduce effective collision frequencies. In a way, the two retarding forces in the momentum equation of positive ions — the convective derivative and the momentum losses — are considered together. By introducing effective collision frequencies, expressions for the ion flux components can be completed in the ordinary form of drift–diffusion fluxes. The validity of the approach is proved in a model of a low pressure argon discharge.

2. Formulation of the problem

Maintenance in a free-fall regime (low gas pressures) of argon discharges is considered. For presenting the procedure for dealing with the nonlinear inertia term in the momentum equation of the ions, *i.e.* the term that specifies the free-fall discharge regime, a simple configuration of the discharge vessel is taken: a rectangular discharge vessel (a parallelepiped) with metal walls. The 2D description presented provides results for the plasma parameters behaviour in the middle (x–z)-plane of the vessel. The shape of the radio frequency (RF) power deposition applied for discharge production is as schematically shown in Fig. 1: homogeneous input power in the x-direction with a super-Gaussian profile

$$P_w(z) = P_{w0} \exp\left[-\frac{1}{2}\left(\frac{z}{\sigma_p}\right)^{2m}\right] \tag{2.1}$$

in the z-direction. Here P_{w0} is the maximum value at $z=0$ and σ_p scales the z-variation.

The initial set of equations includes the continuity equations of electrons and ions ($\alpha = e, i$),

$$\frac{\partial n_\alpha}{\partial t} + \mathrm{div}\boldsymbol{\Gamma}_\alpha = \frac{\delta n_\alpha}{\delta t}, \tag{2.2}$$

the electron energy balance equation

$$\frac{\partial (n_e T_e)}{\partial t} + \mathrm{div}\mathbf{J}_e = P_w + P_{coll}, \tag{2.3}$$

https://doi.org/10.1017/S0022377810000620 Published online by Cambridge University Press

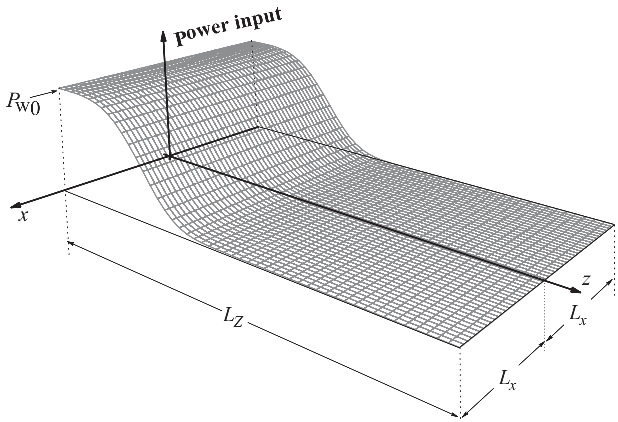

Figure 1. Illustration of the z-variation of the power input.

and the Poisson equation

$$\triangle\Phi = \frac{e}{\varepsilon_0}(n_e - n_i). \tag{2.4}$$

In (2.2)–(2.4), n_α and $\boldsymbol{\Gamma}_\alpha$ are the charged particle densities and fluxes, T_e and $\mathbf{J}_e$ are the electron temperature and the electron energy flux, the latter ($\mathbf{J}_e = \mathbf{J}_{cond} + \mathbf{J}_{conv}$) including both the conductive ($\mathbf{J}_{cond} = -\chi_e \nabla T_e$) and convective ($\mathbf{J}_{conv} = (5/2)T_e\boldsymbol{\Gamma}_e$) fluxes and Φ is the potential of the electric field ($\mathbf{E}_{dc} = -\nabla\Phi$) in the discharge; e is the electron charge, ε_0 is the vacuum permittivity and $\chi_e = (5/2)n_e D_e$, with D_e being the electron diffusion coefficient, is the thermal conductivity coefficient. The charged particle production $\delta n_\alpha/\delta t$ in (2.2) is via direct and step ionization, the latter from the first four excited states considered as a block and the electron energy losses in collisions P_{coll} in (2.3) accounts for elastic and inelastic collisions, the latter for atom excitation taken with a total excitation frequency. The data for the elementary processes are the same as used before [8, 13–15].

The electron flux is a drift–diffusion flux,

$$\boldsymbol{\Gamma}_e = b_e n_e \nabla\Phi - D_e \nabla n_e - D_e^T \nabla T_e, \tag{2.5}$$

including also the thermal diffusion flux. Here $b_e = e/m_e\nu_{ea}$ and $D_e = T_e/m_e\nu_{ea}$ are, respectively, the mobility and diffusion coefficients, with m_e and ν_{ea} being the electron mass and the electron-neutral collision frequency, and $D_e^T = D_e$ is the thermal diffusion coefficient.

The free-fall regime of the discharge maintenance considered requires accounting for the nonlinear inertia term in the momentum equation of the ions. Thus, the latter is taken in its complete form

$$\frac{\partial \mathbf{v}_i}{\partial t} + (\mathbf{v}_i.\nabla)\mathbf{v}_i = -\frac{e}{m_i}\nabla\Phi - \frac{T_i}{m_i n_i}\nabla n_i - \frac{\mu_{in}}{m_i}\nu_{in}\mathbf{v}_i, \tag{2.6}$$

including the convective derivative (the second term on the left-hand side), the drift and diffusion terms (the first two terms on the right-hand side) and the momentum losses in collisions; $\mu_{in} = m_i/2$ is the effective mass in elastic ion-neutral collisions with m_i being the ion mass.

Due to the metal walls of the discharge vessel, the potential of the DC field is fixed to zero there ($\Phi|_{\text{wall}} = 0$). The other boundary conditions are for the fluxes at the walls: $\Gamma_{\text{e}}|_{\text{wall}} = (1/4)n_{\text{e}}v_{\text{the}}$, with v_{the} being the thermal velocity of the electrons, $J_{\text{e}}|_{\text{wall}} = (5/2)T_{\text{e}}\Gamma_{\text{e}}$ and $\Gamma_{\text{i}\perp}|_{\text{wall}} = \Gamma_{\text{i}\perp}|_{\text{pl}}$.

With the DC field accelerating the ions to the walls and the suppressed role of diffusion and collisions at low gas pressures, the nonlinear inertia term in (2.6) grows in importance appearing as the force that limits the ion velocity towards the walls, especially in the wall sheath because of the fast drop of DC potential there. The numerical difficulties, which arise related to the nonlinear inertia term, in the 2D description of discharges with more than one type of positive ions (*e.g.* hydrogen discharges with their three types of positive ions) were the motivation for simplified and reliable procedure for its treatment, as described in the next section.

3. Exact solution and approximations

The results given below are for CW regime maintenance of an argon discharge at gas pressure, $p = 5$ mTorr. The value of the gas temperature is $T_{\text{g}} = 300$ K and the dimensions of the discharge vessel (Fig. 1) are $L_x = 10$ cm and $L_z = 20$ cm. The parameters in the expression for the input power are $m = 2$, $\sigma_{\text{p}} = 4.729$ cm and $P_{\text{w0}} = 10^4$ Wm^{-3}.

First the exact solution of (2.2)–(2.6) is given and then two consecutive approximations are discussed by proving their validity via comparison with the exact solution.

3.1. Exact solution

The exact solutions of (2.2)–(2.6) with account for the nonlinear inertia term in (2.6) in its complete form are given in Figs. 2 and 3 by the curves marked by '(1)'. These present the variations of the electron density (Fig. 2(a)) and temperature (Fig. 2(b)), of the ion velocity (Fig. 2(c)) and of DC potential (Fig. 3(a)) in the transverse (x-) direction (Fig. 1) of the discharge vessel at a position $z = 5$ cm as well as the axial variation of DC potential (Fig. 3(b)) at $x = 0$.

The results show — typical for the free-fall regime maintenance — the formation of well-pronounced wall sheath with sharp drop of the DC potential there (Fig. 3) leading to a strong increase of the ion velocity towards the wall (Fig. 2(c)) and accompanied by a strong drop of the electron density (Fig. 2(a)). Owing to strong thermal conductivity effects, the electron temperature stays almost constant across the discharge (Fig. 2(b)).

Figures 2 and 3 show also the important role of the nonlinear inertia term in the momentum equation of the positive ions for the formation of the entire discharge structure. The curves marked by '(2)' there show the solutions of (2.2)–(2.6) without accounting for the inertia term in (2.6). In fact in this case (2.6) is replaced by an expression for a drift–diffusion flux of ions of the type of expression (2.5). The strong deviation of these results from the exact solutions (curves '(1)') demonstrates the necessity of accounting for the inertia term at low gas pressures. Figure 2(c) also shows the role of the inertia term as a retarding force that limits the increase of ion velocity towards the walls. Without accounting for the inertia term, the ion flux to the walls is overestimated. These overestimated charged particle losses determine,

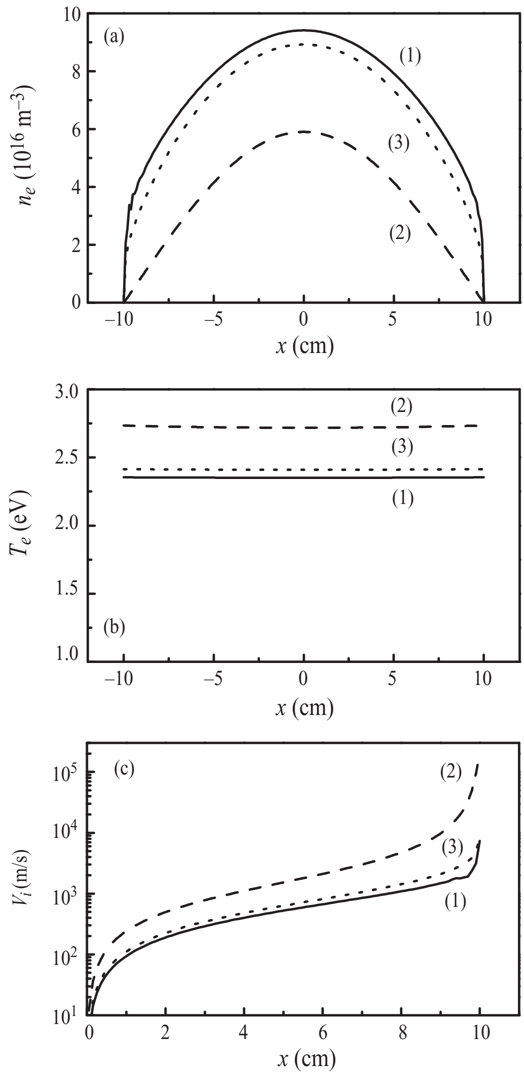

Figure 2. Transverse variations — at $z = 5$ cm — of (a) the electron density, (b) the electron temperature and (c) the ion velocity. The solid curves marked by (1) give the exact solution, with complete account for the inertia term, and the solution obtained with account only for the v_x-velocity component in it. The dashed curves marked by (2) present solutions obtained without accounting for the inertia term. The dot curves marked by (3) show the approximate solution involving the ion energy conservation law.

as it should be expected, higher electron temperature and DC potential and lower plasma density (Figs. 2(a), 2(b) and 3).

Regarding the further suggested approximations to the nonlinear inertia term, Fig. 3 provides important information: the axial and transverse variations of the potential of the DC electric field inside the plasma volume given by the exact solution (curves '(1)') are very slight, determining very weak electric field there. This is confirmed by Fig. 4, which also shows the direction of the electric field. The

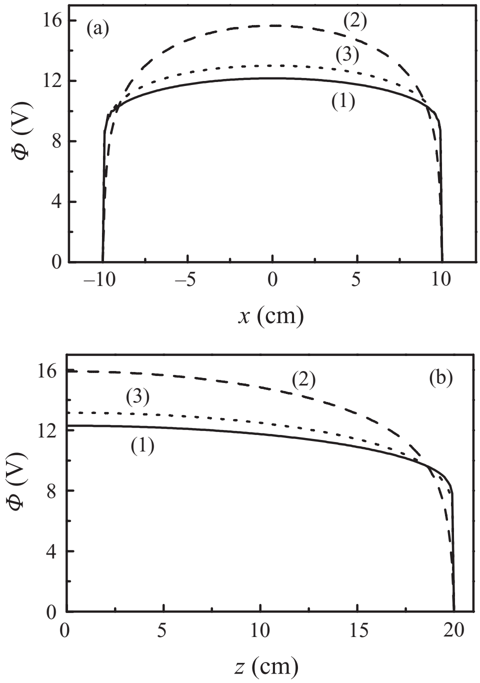

Figure 3. Spatial variation of the potential of the DC electric field in (a) transverse at $z = 5$ cm, and (b) axial at $x = 0$, directions. Curves (1) present both the exact solution, with complete account for the inertia term, and the solution obtained with account only of (a) v_x and (b) v_z velocity component in it. The notation of curves (2) and (3) is the same as in Fig. 2.

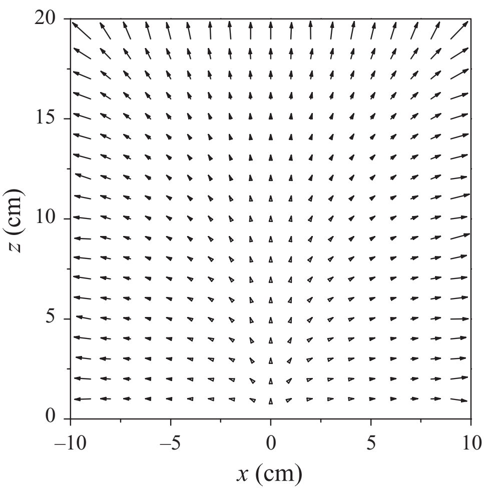

Figure 4. Arrow plot of the DC electric field in the discharge.

https://doi.org/10.1017/S0022377810000620 Published online by Cambridge University Press

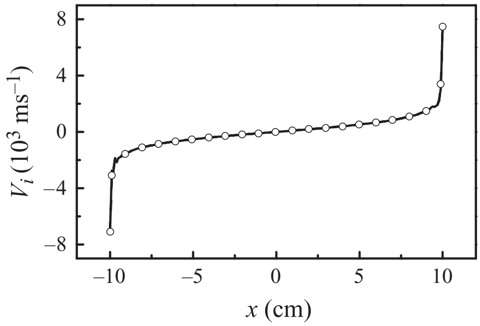

Figure 5. Variation of the transverse component of the ion velocity at $z = 5$ cm obtained as an exact solution (solid curve) and after replacing (2.6) by (3.1)–(3.2) (circles).

electric field is strong only in the wall sheath and its orientation there is almost perpendicular to the walls. This means that the ion velocity increases strongly in the wall sheath, as shown in Fig. 2(c), and is directed towards the corresponding wall of the discharge vessel.

3.2. Approximate solution: disregarding of the parallel — to the walls — velocity component in the inertia term in the ion momentum equation

On the basis of the discussion for the variations of DC potential and for the orientation of DC electric field in the end of the previous sub-section, results for the discharge structure obtained by neglecting — in the inertia term — the parallel (to the corresponding wall) component of the ion velocity are shown here. Thus, (2.6), written for the x- and z- components of the velocity, is reduced to:

$$\frac{\partial v_{\mathrm{ix}}}{\partial t} + v_{\mathrm{ix}}\frac{\partial v_{\mathrm{ix}}}{\partial x} = -\frac{e}{m_{\mathrm{i}}}\frac{\partial \Phi}{\partial x} - \frac{T_{\mathrm{i}}}{m_{\mathrm{i}} n_{\mathrm{i}}}\frac{\partial n_{\mathrm{i}}}{\partial x} - \frac{1}{2}\nu_{\mathrm{in}} v_{\mathrm{ix}} \tag{3.1}$$

$$\frac{\partial v_{\mathrm{iz}}}{\partial t} + v_{\mathrm{iz}}\frac{\partial v_{\mathrm{iz}}}{\partial z} = -\frac{e}{m_{\mathrm{i}}}\frac{\partial \Phi}{\partial z} - \frac{T_{\mathrm{i}}}{m_{\mathrm{i}} n_{\mathrm{i}}}\frac{\partial n_{\mathrm{i}}}{\partial z} - \frac{1}{2}\nu_{\mathrm{in}} v_{\mathrm{iz}}. \tag{3.2}$$

Therefore, from the $(\mathbf{v}.\nabla)\mathbf{v}$-term, $v_{\mathrm{iz}}(\partial v_{\mathrm{ix}}/\partial z)$ and $v_{\mathrm{ix}}(\partial v_{\mathrm{iz}}/\partial x)$ are dropped in (3.1) and (3.2), respectively.

The results for the discharge structure, stemming from (3.1) and (3.2), are given in Figs. 2 and 3 by the same curves '(1)', which show the exact solutions obtained with account for the inertia term in its complete form as given in (2.6). Thus, neglecting the parallel — to the corresponding wall — component of the ion velocity in the nonlinear inertia term does not at all affect the accuracy of the solution. This is also confirmed by Fig. 5, where the exact and approximate solutions for the ion velocity obtained, based respectively on (2.6) and (3.1)–(3.2), are compared in details. The conclusion is that replacing $(\mathbf{v}.\nabla)\mathbf{v}$ by $v_{\mathrm{ix}}(\partial v_{\mathrm{ix}}/\partial x)$ and $v_{\mathrm{iz}}(\partial v_{\mathrm{iz}}/\partial z)$, respectively, in the equation for v_{ix}- and v_{iz}- velocity components could hardly be considered as an approximation. The very good accuracy of the solutions is not only due to having $v_x \gg v_z$ in (3.1) but the spatial derivatives of the velocities also satisfy the inequality $(\partial v_{\mathrm{ix}}/\partial x) \gg (\partial v_{\mathrm{ix}}/\partial z)$. Concerning (3.2), the corresponding inequalities are $v_z \gg v_x$ and $(\partial v_{\mathrm{iz}}/\partial z) \gg (\partial v_{\mathrm{iz}}/\partial x)$.

https://doi.org/10.1017/S0022377810000620 Published online by Cambridge University Press

3.3. *Approximate solution obtained by using the ion energy conservation law in the collisionless case*

The further approximation suggested here provides a possibility for introducing drift–diffusion fluxes of ions still keeping the important part of the inertia term as given by the second terms on the left-hand sides of (3.1) and (3.2).

Considering CW regime and combining the rest of the inertia term in (3.1) and (3.2) with the collisional term therein lead to the following expressions for the ion flux components

$$\Gamma_{\mathrm{ix}} = -b_{\mathrm{ix}}^{\mathrm{eff}} n_{\mathrm{i}} \frac{\partial \Phi}{\partial x} - D_{\mathrm{ix}}^{\mathrm{eff}} \frac{\partial n_{\mathrm{i}}}{\partial x}, \tag{3.3}$$

$$\Gamma_{\mathrm{iz}} = -b_{\mathrm{iz}}^{\mathrm{eff}} n_{\mathrm{i}} \frac{\partial \Phi}{\partial z} - D_{\mathrm{iz}}^{\mathrm{eff}} \frac{\partial n_{\mathrm{i}}}{\partial z}, \tag{3.4}$$

where $b_{\mathrm{i}(x,z)}^{\mathrm{eff}} = e/m_{\mathrm{i}}\nu_{(x,z)}^{\mathrm{eff}}$ and $D_{\mathrm{i}(x,z)}^{\mathrm{eff}} = T_{\mathrm{i}}/m_{\mathrm{i}}\nu_{(x,z)}^{\mathrm{eff}}$ are effective mobilities and diffusion coefficients involving effective collision frequencies via

$$\nu_x^{\mathrm{eff}} = \frac{\partial v_{\mathrm{ix}}}{\partial x} + \frac{1}{2}\nu_{\mathrm{in}}, \tag{3.5}$$

$$\nu_z^{\mathrm{eff}} = \frac{\partial v_{\mathrm{iz}}}{\partial z} + \frac{1}{2}\nu_{\mathrm{in}}. \tag{3.6}$$

With the velocity components included in $\nu_{(x,z)}^{\mathrm{eff}}$, effective collision frequencies are specified for each direction. In a way, the two retarding forces — the collisional term and the inertia term — are considered together, combined in effective collision frequencies.

Up to this point, no approximations have been done: Expressions (3.3) and (3.4) results directly from (3.1) and (3.2). The approximation suggested further concerns the determination of the rest of the inertia term included in (3.5) and (3.6), *i.e.* the first terms on the right-hand sides therein. The stationary form of (3.1) and (3.2) written without the collisional and diffusion terms results in the energy conservation law,

$$\frac{1}{2} m_{\mathrm{i}} v_{\mathrm{i}(x,z)}^2 = e(\Phi_{\max} - \Phi), \tag{3.7}$$

where $\Phi_{\max} = \Phi(x=0, z=0)$. Thus, the spatial derivatives of the velocity components present in (3.5) and (3.6) can be expressed as

$$\frac{\partial v_{\mathrm{ix}}}{\partial x} = -\sqrt{\frac{e}{2m_{\mathrm{i}}}} \frac{\frac{\partial \Phi}{\partial x}}{\sqrt{\Phi_{\max} - \Phi}}, \tag{3.8}$$

$$\frac{\partial v_{\mathrm{iz}}}{\partial z} = -\sqrt{\frac{e}{2m_{\mathrm{i}}}} \frac{\frac{\partial \Phi}{\partial z}}{\sqrt{\Phi_{\max} - \Phi}}. \tag{3.9}$$

In a way, the effective collision frequencies (3.5) and (3.6) and, respectively, the ion flux components (3.3) and (3.4) needed for the continuity expression (2.2) are obtained in an explicit form. The results obtained as solutions of (2.2)–(2.5), (3.3)–(3.6), (3.8) and (3.9) are shown by the curves marked by '(3)' in Figs. 2 and 3.

As Fig. 2 and 3 show, the variation in the transverse direction of the electron density (Fig. 2(a)) and temperature (Fig. 2(b)) and of the ion velocity (Fig. 2(c)), as well as the variations of the plasma potential both in the transverse and longitudinal directions (Fig. 3) are very close to the corresponding exact solutions (curves '(1)'). Thus, expressions (3.8) and (3.9) obtained from the ion energy conservation law written in the collisionless case appear as a good approximation to the spatial derivatives of the ion velocity components present in the inertia term and, respectively, in the effective collision frequencies (3.5) and (3.6). The good accuracy of the results may be attributed to the fact that the approximation concerns only the derivative in the inertia term, and not the entire term.

With the effective increase of the collisional frequency caused by the inertia term, the discharge behaves as a discharge at an effective – higher – gas pressure: the electron temperature and the potential of the DC field are lower and the plasma density is higher compared to the case when the inertia term is neglected (curves '(2)' in Figs. 2 and 3).

4. Conclusions

A simplified procedure shown to be with very good accuracy is suggested for dealing with the nonlinear inertia term in the momentum equation of the positive ions in the 2D modelling of free-fall regime-sustained discharges. The procedure involves two consecutive approximations. Neglecting the parallel – with respect to the given wall – component of the ion velocity is the first approximation shown not to affect at all the accuracy of the solutions for the discharge structure. The reason is that the nonlinear inertia term grows in importance in the wall sheaths where the DC electric field is almost perpendicular to the walls. The second approximation involves the ion-energy conservation law for the determination of spatial derivative of the corresponding velocity component in the rest of the inertia term. In a way, the inertia term is expressed in an explicit form and combined with the collisional term, resulting in the introduction of effective collision frequencies. This permits description of the free-fall regime maintenance via the ordinary procedure based on drift–diffusion fluxes. The validity of the procedure is proved based on a 2D model of argon discharges.

Acknowledgements

The work is within project DO02-267 supported by the National Science Fund in Bulgaria and is part of the work on task P2 of the programme of the Bulgarian Association EURATOM/INRNE.

References

[1] Tonks, L. and Langmuir, I. 1929 *Phys. Rev.* **34**, 876.

[2] Self, S. A. and Ewald, H. N. 1966 *Phys. Fluids* **9**, 2486.

[3] Self, S. A. 1967 *Phys. Fluids* **10**, 1569.

[4] Ilić, D. B. 1973 *J. Appl. Phys.* **44**, 3993.

[5] Kouznetsov, I. G., Lichtenberg, A. J. and Lieberman, M. A. 1996 *Plasma Sources Sci. Technol.* **5**, 662.

[6] Franklin, R. N. 2000 *Plasma Sources Sci. Technol.* **9**, 191.

[7] Pejović, M. M., Ristić, G. S. and Karamaković, J. P. 2002 *J. Phys. D: Appl. Phys.* **35**, R91.

[8] Paunska, Ts., Shivarova, A. and Tarnev, Kh. 2004 *Vacuum* **76**, 377.

[9] Paunska, Ts., Schlüter, H., Shivarova, A. and Tarnev, Kh. 2006 *Phys. Plasmas* **13**, 023504.
[10] Salabas, A., Gousset, G. and Alves, L. L. 2002 *Plasma Sources Sci. Technol.* **11**, 448.
[11] Richards, A. D., Thompson, B. E. and Sawin, H. H. 1987 *Appl. Phys. Lett.* **50**, 492.
[12] Gogolides, E. and Sawin, H. H. 1992 *J. Appl. Phys.* **72**, 3971.
[13] Makasheva, K. and Shivarova, A. 2001 *Phys. Plasmas* **8**, 836.
[14] Kolev, St., Schlüter, H., Shivarova, A. and Tarnev, Kh. 2006 *Plasma Sources Sci. Technol.* **15**, 744.
[15] Kolev, St., Lishev, St., Shivarova, A., Tarnev, Kh. and Wilhelm, R. 2007 *Plasma Phys. Control. Fusion* **49**, 1349.